Oxidation-State-Dependent Protein Docking between Cytochrome *c* and Cytochrome b_5: High-Pressure Laser Flash Photolysis Study†

Yoshiaki Furukawa, Koichiro Ishimori, and Isao Morishima*

Department of Molecular Engineering, Graduate School of Engineering, Kyoto University, Kyoto 606-8501, Japan

Received March 7, 2002; Revised Manuscript Received May 30, 2002

ABSTRACT: To characterize the protein−protein interaction during electron transfer, we used Zn-substituted cytochrome *c* (ZnCyt*c*) as a model of ferrous Cyt*c* and determined the volume change, ΔV_d^{Zn}, for the dissociation of its complex with ferric cytochrome b_5 (Cytb_5) by the pressure dependence of its photoinduced electron-transfer kinetics. Under ambient pressure, the dissociation constant, K_d^{Zn}, of the ZnCyt*c*/Cytb_5 complex was dependent on the buffer concentration, 1.5 and 12 μM in 2 and 10 mM Tris-HCl, pH 7.4, respectively, which was consistent with formation of salt bridges in its complexation. The dissociation of one salt bridge is usually associated with large volume changes of −10 to −30 cm^3 mol^{-1}, while pressure dependence of K_d^{Zn} resulted in smaller value of ΔV_d^{Zn}, −8.5 cm^3 mol^{-1}. Therefore, the interaction between ZnCyt*c* and Cytb_5 cannot be explained only by salt bridge interaction, and the partial cancellation by the positive volume change due to the additional hydrophobic interaction is a plausible explanation for the observed ΔV_d^{Zn}. In addition, ΔV_d^{Zn} of −8.5 cm^3 mol^{-1} was considerably smaller than the previously reported volume change, ΔV_d^{Fe}, of −122 cm^3 mol^{-1} in the ferric Cyt*c*/Cytb_5 complex dissociation [Rodgers and Sligar (1991) *J. Mol. Biol. 221,* 1453−1460]. ZnCyt*c* used here has been assumed to be a reliable model of ferrous Cyt*c*, and thus the discrepancy between our present ΔV_d^{Zn} and the previous ΔV_d^{Fe} is discussed on the basis of the protein docking dependent on the oxidation states of heme iron in Cyt*c*.

Electron transfer (ET)[1] reactions play essential roles in the biological important processes such as photosynthesis and respiration and typically involve the transport of electrons through a series of distinct protein−protein complexes (*1*, *2*). For maintenance of the physiological specificity in transferring an electron, the molecular recognition is requisite between redox proteins. The characterization of protein−protein interactions involved in ET reactions is, therefore, a fundamental step for the comprehension of the molecular recognition mechanism.

One of the most widely studied systems for protein−protein interactions is a pair between cytochromes *c* (Cyt*c*) and b_5 (Cytb_5) (*3*, *4*). The structural characterization of the complex between ferric Cyt*c* and ferric Cytb_5 has been vigorously attempted by theoretical and experimental approaches, including computer simulation (*5*−*7*), chemical modification (*8*, *9*), and site-directed mutagenesis (*10*−*12*). In these previous studies, the salt bridge interactions have been recognized as the crucial factor for the ferric Cyt*c*/ferric Cytb_5 complexation. In particular, the volume change upon the complex dissociation, ΔV_d, has been a useful thermodynamic quantity to characterize protein−protein interaction sites. Upon dissociation of protein complexes, the exposure of the charged groups to solvent results in an electrostriction of the solvent, which contributes to a corresponding decrease in the overall volume of system (−10 to −30 cm^3 mol^{-1}) (*13*, *14*). Rodgers and Sligar (*15*, *16*) have reported the large volume decrease, −122 cm^3 mol^{-1}, upon the dissociation of the ferric complex between horse heart Cyt*c* and rat hepatic Cytb_5 in the solution condition of 2 mM Tris-HCl, pH 7.4. In combination with the site-directed mutagenesis, Rodgers and Sligar (*16*) have further proposed that the observed ΔV_d, −122 cm^3 mol^{-1}, can be well explained by the so-called Salemme model (*17*) with the four salt bridge interactions (Figure 1).

The complex formed in ET reactions contains a pair of the reduced and oxidized states of the individual cytochromes, which are well-known to change the structure and its dynamics in response to the oxidation state of its active site, heme. In particular, the structural difference between ferric and ferrous Cyt*c* has been discussed by using various spectroscopic techniques (*18*−*23*), and the interactions of Cyt*c* with its redox partners such as Cyt*c* oxidase (*24*) or Cyt*c* peroxidase (*25*) have also been argued in reference to the oxidation states of the cytochromes. Therefore, the ET reaction between Cyt*c* and Cytb_5 would not necessarily proceed in the binding geometry, as seen in the ferric pair of the cytochromes. Indeed, several structural models of the Cyt*c*/Cytb_5 complex have been proposed on the basis of the computer simulations (*5*−*7*, *10*, *26*), implying the sites other than the Salemme model are also amenable to the complex-

† This work was supported by a grant from Ministry of Education, Science, Culture, and Sports (to I.M., No.12002008). Y.F. was supported by Research Fellowships of the Japan Society for the Promotion of Science for Young Scientists.

* To whom correspondence should be addressed. Phone: +81-75-753-5921. Fax: +81-75-751-7611. E-mail: morisima@mds.moleng.kyoto-u.ac.jp.

[1] Abbreviations: ET, electron transfer; Cyt*c*, cytochrome *c*; Cytb_5, cytochrome b_5; porphyrin-Cyt*c*, metal-depleted porphyrin-substituted cytochrome *c*; ZnCyt*c*, Zn-substituted cytochrome *c*; ^{3}ZnCyt*c**, triplet-excited state of Zn-substituted cytochrome *c*; SDS, sodium dodecyl sulfate; D−A distance, the distance between electron donor and acceptor.

10.1021/bi0257890 CCC: $22.00
Published on Web 07/12/2002

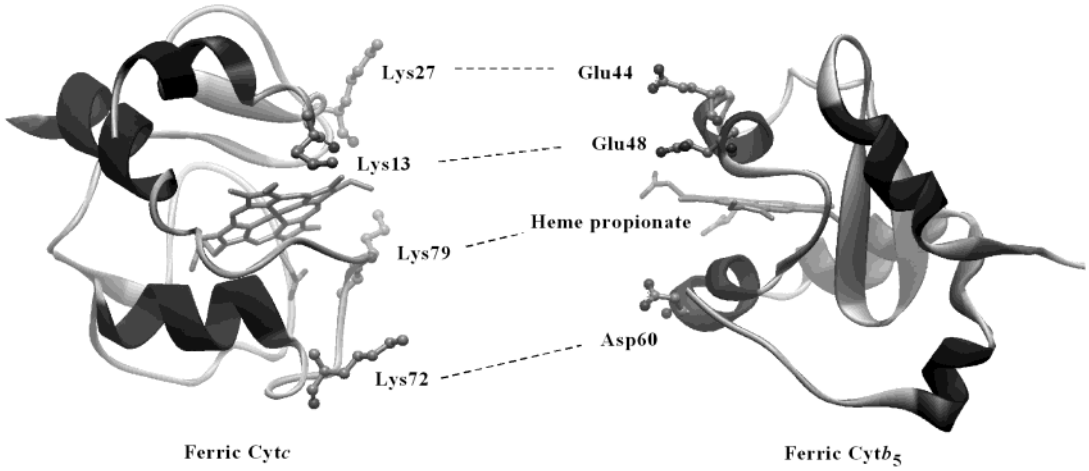

FIGURE 1: Salt bridge interactions in the complex between Cyt*c* and Cytb_5 proposed by Salemme (*17*). The dotted lines indicate pairs of the salt bridges.

ation. However, it has not been experimentally examined whether the interaction between these two cytochromes is affected by the oxidation states of the heme iron ion.

To address the protein−protein interactions dependent upon the oxidation states of the cytochrome, we investigated the pressure dependence of the dissociation between Zn-substituted Cyt*c* (ZnCyt*c*) and Cytb_5. The structural characterization of ZnCyt*c* has suggested that replacement of iron (II) by zinc (II) does not perturb the conformation of Cyt*c* and its association with the redox partner (*27*). Using ZnCyt*c* as the reliable model of ferrous Cyt*c*, we evaluated the dissociation constant from the photoinduced ET reactions from ZnCyt*c* to Cytb_5. As reported by Qin and Kostić (*28*), the laser-generated triplet-excited state of ZnCyt*c* can transfer an electron to Cytb_5, resulting in its decay to the ground state. Out of the total decay amplitude, the fraction occupied by the intracomplex ET process, of which the rate constant is independent of the Cytb_5 concentration, indicates the degree of the complexation between ZnCyt*c* and Cytb_5. The volume change upon the dissociation of the ZnCyt*c*/Cytb_5 complex can be further examined from the pressure dependence of the ET kinetics between ZnCyt*c* and Cytb_5. Comparing it with the volume change previously reported in the ferric pair of the cytochromes (*16*), we discussed the protein docking between Cyt*c* and Cytb_5 in relation to the oxidation states of Cyt*c*.

EXPERIMENTAL PROCEDURES

Protein Preparation. Cytb_5 was prepared as reported previously (*29*). *Escherichia coli* TB-1 cells containing the plasmid, pUC13, which harbors the gene for the soluble heme-containing domain of rat hepatic Cytb_5, were grown in 2xTY culture overnight. The finally purified Cytb_5 protein gave a single band on SDS polyacrylamide gels and the A_{413}/A_{280} ratio of 5.8 and was stored at −80 °C.

Substitution of zinc ion for iron ion in Cyt*c* was performed as published elsewhere (*30*). In short, iron bound to the heme group in Cyt*c* was removed by reaction with anhydrous hydrogen fluoride, resulting in the formation of porphyrin-Cyt*c*. Horse heart Cyt*c* (100 mg), purchased from Wako chemicals, was dissolved in 2 mL of hydrogen fluoride in a Teflon tube dipped in dry ice/ethanol at −70 °C. The protein solution was stirred for 5−10 min, and it was dried under negative pressure on ice for 1 h. The dried protein was gently dissolved in ca. 10 mL of 50 mM ammonium acetate, 6 M Gdn-HCl, pH 5.0. After the concentration of the solution to ca. 1 mL by using Centrifugal Filter Device (Millipore), the crude porphyrin-Cyt*c* was loaded onto the PD-10 gel filtration column (Amersham Pharmacia Biotech), which was preequilibrated with 50 mM ammonium acetate and pH 5.0. The 15-fold excess of zinc acetate (56.6 mg) was added to the porphyrin-Cyt*c* solution (20 mL, 0.9 mM), and the mixture was kept in a water bath at 50 °C for 30 min in dark to reconstitute zinc ion into porphyrin-Cyt*c*. Crude ZnCyt*c* was further purified by a HiTrapSP cation-exchange column fitted to the Pharmacia FPLC system. The samples were loaded on the column equilibrated with 50 mM Na−Pi, pH 7.1, and eluted with a linear gradient of 50 mM Na−Pi, 500 mM NaCl, and pH 7.0.

Laser Flash Photolysis. The second harmonic (532 nm) of a Q-switched Nd:YAG laser provided photolysis pulses with a half peak duration of 10 ns. The monitoring beam was generated by a xenon lamp (150 W) and focused on the sample cell at the right angle of the excitation source. The transmitted light was detected by a photomultiplier that is attached on a monochromator, UNISOKU USP-501. A two-channel oscilloscope (TDS520) was used to digitize, and the accumulated signals were transferred to a NEC PC-98 computer for the further analysis. High-pressure laser flash photolysis measurements were performed using the high-pressure cell (PCI-400) developed by TERAMECS Co. Ltd. The pressure was transmitted from a high-pressure hand pump (TP-500, TERAMECS) and was measured by a Bourdon tube over a range from atmospheric pressure to 200 MPa. Temperature was controlled by using a circulating water bath. Each rate constant reported in this study is the average of 20 individual kinetic measurements at the stated pressure. The transient absorbance changes of ^{3}ZnCyt*c** were monitored at 460 nm (*28*). The concentration of ZnCyt*c* was kept at 7 μM, and Cytb_5 was titrated from 5 to 25 μM. The high-pressure laser flash photolysis measurements were usually performed at pressure intervals of 50 to 200 MPa. After lowering the pressure to 0.1 MPa, we confirmed the decay kinetics of ^{3}ZnCyt*c** in the presence of Cytb_5 to be the same as that before raising the pressure within the experimental error, which further shows that pressure does

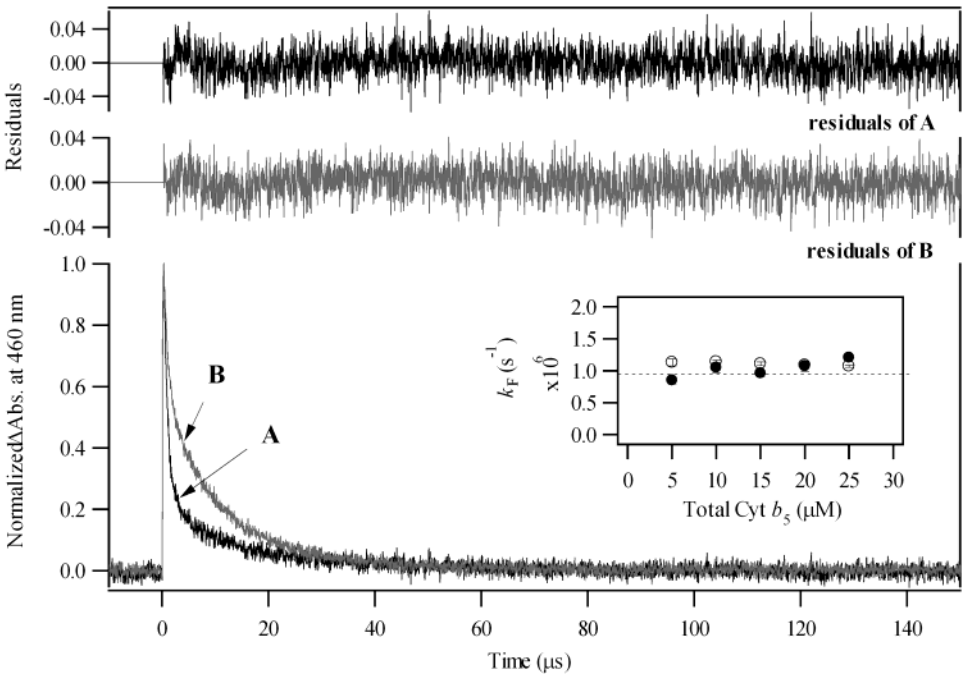

FIGURE 2: Normalized transient absorbance changes at 460 nm obtained after laser excitation of 7 μM ZnCyt*c* with 15 μM Cytb_5 (A) in 2 mM Tris-HCl, pH 7.4, and (B) in 10 mM Tris-HCl, pH 7.4, at 293 K. The residuals of the single-exponential fitting are shown on the top. (inset) The dependence of the rate constant, k_F, on the Cytb_5 concentration. Open circles indicate the rate constants measured under 2 mM Tris-HCl, pH 7.4, while black circles are under 10 mM Tris-HCl, pH 7.4.

Scheme 1

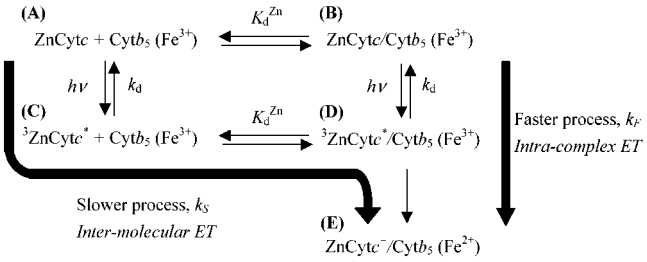

not induce the irreversible denaturation of the proteins. All experiments were performed in Tris-HCl buffer, since the pH of Tris buffer has been shown to be independent of pressure up to 200 MPa (*31*).

RESULTS

Kinetics under Ambient Pressure. The quenching of ^{3}ZnCyt*c** by ferric Cytb_5 has already been examined by Qin and Kostić (*28*) and other investigators (*32*, *33*) under ambient pressure and confirmed as the ET process from ^{3}ZnCyt*c** to ferric Cytb_5. Qin and Kostić (*28*) have also reported that the observed ET quenching process of ^{3}ZnCyt*c** by Cytb_5 can be explained by the two exponential functions based upon Scheme 1, the intermolecular ET of ^{3}ZnCyt*c** by Cytb_5 and the intracomplex ET in the preformed ZnCyt*c*/Cytb_5 complex. Consistent with their results, we observed that the absorbance decay of ^{3}ZnCyt*c**, ΔA, in the presence of ferric Cytb_5 can be well fitted by two exponential functions with the rate constants, k_F and k_S (eq 1)[2]

$$\Delta A = a_1 \exp(-k_F t) + a_2 \exp(-k_S t) + a_3 \qquad (1)$$

where a_1 and a_2 are the amplitudes of the individual exponential decay processes. The constant, a_3, in eq 1 means the final absorbance to which ^{3}ZnCyt*c** decays. Although a_3 will be ideally zero (Scheme 1), in the current experiments a_3 amounts to less than 1% of total decay amplitude because of the noisy signal of the transient absorbance changes. Typical decay kinetics observed at 460 nm after a laser pulse is shown in Figure 2A. The random residuals were obtained in the fitting of the decay by eq 1 (top of Figure 2), which confirms that the decay of ^{3}ZnCyt*c** consisted of the two kinetic phases.

Under the buffer condition of 10 mM Tris-HCl, pH 7.4, the rate constant, k_S, for the slower kinetic phase (amplitude a_2) is linearly dependent upon the Cytb_5 concentration (See Figure S1 in Supporting Information), indicating the bimolecular quenching process of ^{3}ZnCyt*c** by Cytb_5. When the buffer concentration (the ionic strength of solution) was lowered to 2 mM Tris-HCl, pH 7.4, k_S showed the saturation

[2] As reported previously, dissolved oxygen in the sample also quenches the triplet-excited state of Zn-substituted hemoproteins and accelerates the observed decay kinetics. In the absence of ferric Cytb_5, the ^{3}ZnCyt*c** decay rate constant, k_d, was actually about 10-fold accelerated, 70 and 800 s^{-1} under anaerobic and aerobic conditions, respectively. In the presence of ferric Cytb_5, however, the decay rate of ^{3}ZnCyt*c** was barely affected by oxygen, which would be due to the 10^2-10^4-fold faster ET rate to Cytb_5 compared to k_d under aerobic condition, 800 s^{-1}. Accordingly, even in the presence of the dissolved oxygen, ^{3}ZnCyt*c** will decay preferentially through the ET process to Cytb_5, and we confirmed, in this study, virtually the same decay kinetics under aerobic and anaerobic conditions.

[3] For calculation of the net charge and the dipole moment of Cyt*c*, we used the computer program, MacroDox ver. 3.2.2, developed by Northrup et al. (*10*)

[4] To further examine the interactions of ferric Cyt*c* with ferrous Cytb_5 by the ET kinetics and quantify its volume change, we have also constructed Zn-substituted Cytb_5 (ZnCytb_5) and attempted to evaluate the pressure dependence of the photoinduced ET reaction of ZnCytb_5 with ferric Cyt*c*. However, the structural characterization by the circular dichroism spectroscopy suggested that ZnCytb_5 has the apo-like conformation of Cytb_5 (Furukawa et al. unpublished), which hampers the further discussion on the protein−protein interactions in the ferric Cyt*c*/ferrous Cytb_5 complex.

behavior against the Cytb_5 concentration (See Figure S1 in Supporting Information). Decrease of the ionic strength is led to reinforce the electrostatic interactions between ZnCyt*c* and Cytb_5 (*28*), and the saturation kinetics of the slower phase is also consistent with the bimolecular quenching of ^{3}ZnCyt*c** by Cytb_5 following the complex formation (A → C → D → E in Scheme 1).

On the other hand, the rate constant, k_F, for the faster phase (amplitude a_1) was independent of the Cytb_5 concentration (5−25 μM) and estimated as 1.0×10^6 s^{-1}, which is independent of the buffer concentration (2−10 mM Tris-HCl, inset of Figure 2). The observed k_F is in agreement with the previous results by Qin and Kostić (*28*), and it is considered that the faster phase corresponds to the intracomplex quenching of ^{3}ZnCyt*c** by ferric Cytb_5 in the preformed ZnCyt*c*/Cytb_5 complex before the excitation of ZnCyt*c* by a laser shot (B → D → E in Scheme 1). The amplitudes, a_1 and a_2, parallel the amounts of the preformed complex (state B in Scheme 1) and the free state (state A in Scheme 1) of ZnCyt*c*, respectively, and these decay amplitudes can further afford the estimation of the dissociation constant.

To calculate the dissociation constant, K_d^{Zn}, of the ZnCyt*c*−Cytb_5 complex, we noted the fraction of the faster phase, $a_1/(a_1+a_2)$, in the total decay amplitude, by which the preformed complex state (ZnCyt*c*/Cytb_5 (Fe^{3+}), state B in Scheme 1) can be quantified (eq 2)

$$\frac{a_1}{a_1 + a_2} = \frac{[\text{ZnCyt}c/\text{Cyt}b_5]}{[\text{ZnCyt}c] + [\text{ZnCyt}c/\text{Cyt}b_5]} \qquad (2)$$

Because the contribution of a_3 to the total decay amplitude was less than 1%, it is not necessary to be taken into account for the determination and the analysis of K_d^{Zn}. As shown in Figure 3, the fraction, $a_1/(a_1+a_2)$, showed the saturation behavior with increase of the Cytb_5 concentration. It has been known that ZnCyt*c* and Cytb_5 exhibit simple 1:1 binding scheme (*3*), and the dissociation constant, K_d^{Zn}, can be defined as eq 3

$$K_d^{Zn} = \frac{[\text{ZnCyt}c][\text{Cyt}b_5]}{[\text{ZnCyt}c/\text{Cyt}b_5]} \qquad (3)$$

Using eqs 2 and 3, the fraction, $a_1/(a_1+a_2)$, can be expressed by K_d^{Zn} as described in eq 4

$$\frac{a_1}{a_1 + a_2} = \frac{[\text{ZnCyt}c]_t + [\text{Cyt}b_5]_t + K_d^{Zn} - \sqrt{([\text{ZnCyt}c]_t + [\text{Cyt}b_5]_t + K_d^{Zn})^2 - 4[\text{ZnCyt}c]_t[\text{Cyt}b_5]_t}}{2[\text{ZnCyt}c]_t} \qquad (4)$$

In this equation, $[\text{ZnCyt}c]_t$ and $[\text{Cyt}b_5]_t$ indicate the total concentrations of ZnCyt*c* and Cytb_5 dissolved in the sample solution, respectively. In the solution condition of 2 mM Tris-HCl, pH 7.4, the fitting of the data (Figure 3A, open circles) to eq 4 resulted in K_d^{Zn} of 1.5 ± 0.1 μM.

We also investigated effects of ionic strength in solution on the dissociation constant, K_d^{Zn}, to examine electrostatic interactions in the complexation between ZnCyt*c* and Cytb_5. As mentioned in the Introduction, the electrostatic interactions have been suggested to play important roles in the Cyt*c*/Cytb_5 complexation. In the higher ionic strength condition, 10 mM Tris-HCl and pH 7.4, the fraction, $a_1/(a_1+a_2)$, was smaller than that in the buffer condition of 2 mM Tris-HCl (Figure 3B) and can be fitted to eq 4 with the dissociation constant of 12 ± 1.6 μM. Compared to K_d^{Zn} under 2 mM Tris-HCl, the approximately 10-fold reduced affinity in the increased ionic strength solution (10 mM Tris-HCl) suggests the relevance of the electrostatic interactions in the complex formation between ZnCyt*c* and Cytb_5.

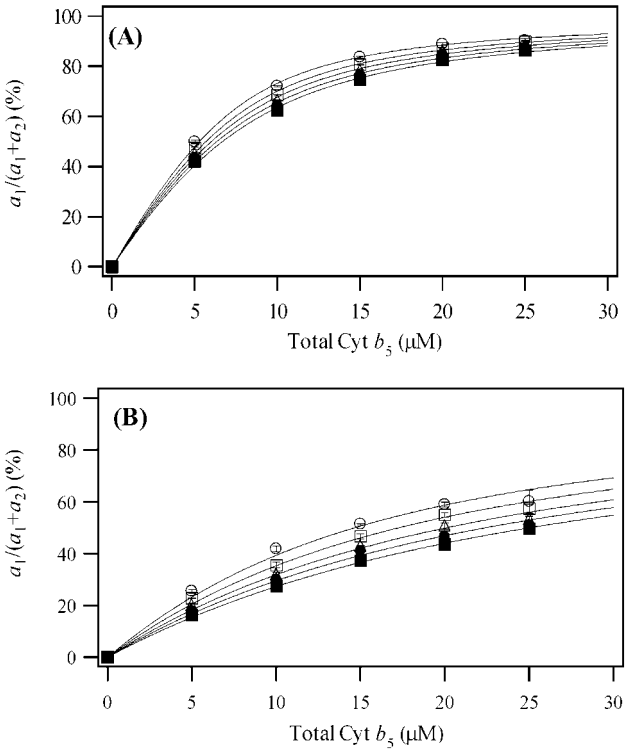

FIGURE 3: Dependence of the fraction of the faster phase, $a_1/(a_1+a_2)$, on the Cytb_5 concentration (A) in 2 mM Tris-HCl, pH 7.4, or (B) in 10 mM Tris-HCl, pH 7.4. The pressure was as follows: 0.1 (open circle), 50 (open square), 100 (open triangle), 150 (filled circle), and 200 MPa (filled square). The solid curves are the least-squares fits by eq 4.

Kinetics under Higher Pressure. We have further examined the pressure dependence of the intracomplex ET quenching process, $a_1 \exp(-k_F t)$ in eq 1, up to 200 MPa with an interval of 50 MPa so as to gain an insight into the effects of pressure on ZnCyt*c*/Cytb_5 complexation process. Under higher pressures up to 200 MPa, the decay kinetics of ^{3}ZnCyt*c** quenched by ferric Cytb_5 consisted of the two phases (Figure 4), and the rate constant of the faster phase, k_F, remains independent of the Cytb_5 concentration (data not shown), indicating that the faster phase under higher pressure also expresses the intracomplex ET process. The fraction of the fast process, $a_1/(a_1+a_2)$, was significantly decreased under higher pressure (Figure 3), indicating that the ZnCyt*c*/Cytb_5 complex tends to dissociate by pressurization. The volume change, ΔV_d^{Zn}, in the dissociation of the ZnCyt*c*/Cytb_5 complex was estimated for the quantitative analysis by the following equation:

$$\left(\frac{\partial \ln K_d^{Zn}}{\partial P}\right)_T = -\frac{\Delta V_d^{Zn}}{RT} \qquad (5)$$

The plot of the natural logarithm of K_d^{Zn} against pressure

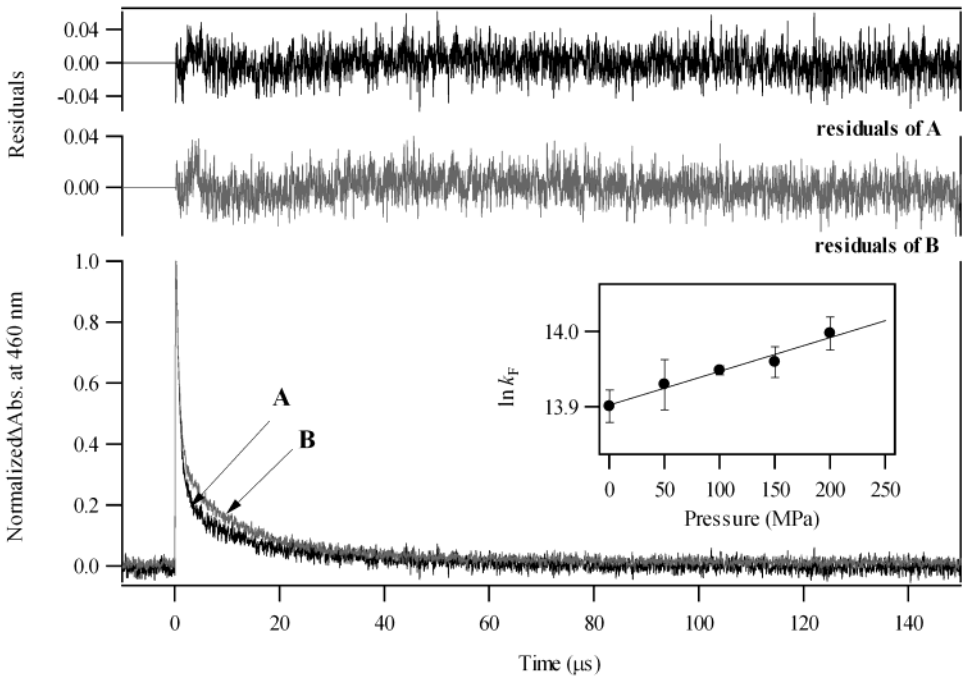

FIGURE 4: Normalized transient absorbance changes at 460 nm obtained after laser excitation of 7 μM ZnCyt*c* with 15 μM Cytb_5 at (A) 0.1 and (B) 200 MPa in 2 mM Tris-HCl, pH 7.4, 293 K. The residuals of the double-exponential fitting are shown on the top. (inset) The typical pressure dependence of intracomplex ET rate, k_F, in the pair of ZnCyt*c* and Cytb_5. The data on this inset are taken in the condition of 7 μM ZnCyt*c* with 15 μM Cytb_5 in 2 mM Tris-HCl, pH 7.4.

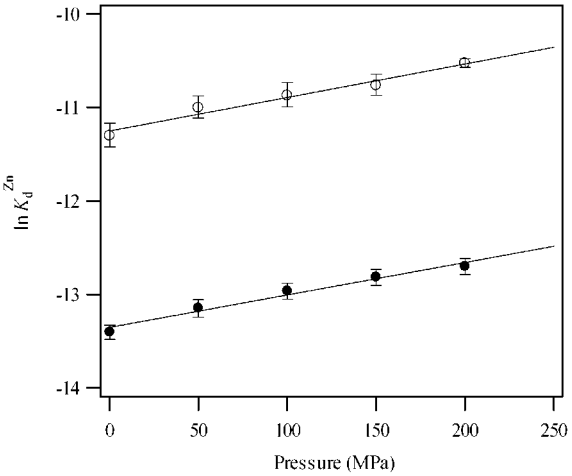

FIGURE 5: Pressure dependence of the dissociation constant between ZnCyt*c* and Cytb_5 estimated from the fraction of the faster kinetic phase (Figure 4) in (filled circles) 2 mM Tris-HCl, pH 7.4, and (open circles) 10 mM Tris-HCl, pH 7.4. Solid lines are linear least-squares fits.

was linear (Figure 5), and the volume change for the dissociation was determined by the linear least-squares fitting; $\Delta V_d^{Zn} = -8.5 \pm 0.8$ and -8.7 ± 0.9 cm^3 mol^{-1} under 2 and 10 mM Tris-HCl, pH 7.4, respectively. While changes of ionic strength can lead to perturbation of the Cyt*c* structure (*21*) and might affect the binding geometry with Cytb_5, the ionic strength-independent ΔV_d^{Zn} observed here implies that the ZnCyt*c*/Cytb_5 complex has the same structure in the range from 2 to 10 mM Tris-HCl.

Prior to the detailed discussion on ΔV_d^{Zn}, it would be necessary to reveal that pressurization does not perturb the binding site. As previously reported by us (*34*) and another group (*35*), the pressure dependence of the ET rate constants in proteins afford the changes in the D−A distance (Zn-porphyrin in ZnCyt*c* and heme in Cytb_5) with pressurization. Because the protein−protein binding site in its complex affects the D−A distance (*1*), the analysis of the D−A distance change with pressurization can provide information on the binding site in the ZnCyt*c*/Cytb_5 complex under higher pressure. For the quantitative analysis of the D−A distance change under higher pressure, we introduced the activation volume, $\Delta V^{\ddagger}$, as the following equation:

$$\left(\frac{\partial \ln k_F}{\partial P}\right)_T = -\frac{\Delta V^{\ddagger}}{RT} \tag{6}$$

where P is the pressure, R is the gas constant, and T is the temperature. The rate constant, k_F, showed the slight acceleration against the pressurization, and the plot of the natural logarithm of k_F against the pressure was linear (inset of Figure 4). The activation volume, $\Delta V^{\ddagger}$, for the intracomplex ET at each Cytb_5 concentration was determined by the linear least-squares fitting: -1.0 ± 0.3, -1.5 ± 0.3, -1.5 ± 0.1, -1.1 ± 0.1, and -0.8 ± 0.3 cm^3 mol^{-1} at 5, 10, 15, 20, and 25 μM of the Cytb_5 concentration, respectively. $\Delta V^{\ddagger}$ does not appear to be dependent upon the Cytb_5 concentration, and we used its averaged value, -1.2 ± 0.2 cm^3 mol^{-1}, for further analysis.

On the basis of our previous study (*34*), the activation volume, $\Delta V^{\ddagger}$, for the ET rate constants, k, can be expressed as eq 7 using the Marcus equation (eq 8) (*1*):

$$\Delta V^{\ddagger} = \beta RT\left(\frac{\partial d}{\partial P}\right)_T + \left(\frac{\Delta G^{\circ} + \lambda}{2\lambda}\right)\left(\Delta V_{^3ZnCytc^* \rightarrow ZnCytc^+} + \Delta V_{Cytb_5(Fe^{3+}) \rightarrow Cytb_5(Fe^{2+})}\right) \tag{7}$$

$$k = 10^{13} \exp[-\beta(d-3)] \exp\left[-\frac{(\Delta G^{\circ} + \lambda)^2}{4\lambda RT}\right] \tag{8}$$

where β and λ are distance decay factor and reorganization energy, respectively. $\Delta G°$ is the redox potential difference between the redox cofactors at ambient pressure. In eq 7, the activation volume, $\Delta V^{\ddagger}$, for the ET reactions can be illustrated by the pressure-induced change of the D−A distance, *d*, and the volume change of the redox centers, $\Delta V_{^3\text{ZnCyt}c^* \rightarrow \text{ZnCyt}c^+}$ and $\Delta V_{\text{Cyt}b_5(Fe^{3+}) \rightarrow \text{Cyt}b_5(Fe^{2+})}$. It has been suggested (*34*, *36*−*38*) that the volume changes of heme or Zn-porphyrins are rather small; therefore, $\Delta V_{^3\text{ZnCyt}c^* \rightarrow \text{ZnCyt}c^+} + \Delta V_{\text{Cyt}b_5(Fe^{3+}) \rightarrow \text{Cyt}b_5(Fe^{2+})}$ is approximately 0 cm^3 mol^{-1} in eq 7. Because the ET system between ^{3}ZnCyt*c** and Cytb_5 exhibits $\Delta G°$ and λ of −0.8 and 0.8 eV, respectively (*32*), the term, $(\Delta G° + \lambda)/2\lambda$, in eq 7 would be nearly equal to zero. Upon the basis of these assumptions, the equation for $\Delta V^{\ddagger}$ in the ET reaction between ZnCyt*c* and Cytb_5 can be reduced to the following equation:

$$\Delta V^{\ddagger} = \beta RT\left(\frac{\partial d}{\partial P}\right)_T \qquad (9)$$

To evaluate the distance change under high pressure, we applied 1.4 Å^{-1} for the value of β, which has been encountered for many protein ET systems (*39*). Using the observed value of -1.2 ± 0.2 cm^3 mol^{-1} for the activation volume, $\Delta V^{\ddagger}$, eq 9 shows that the distance change by pressurization, $(\partial d/\partial P)_T$, was $(-3.5 \pm 0.6) \times 10^{-4}$ ÅMPa^{-1}. This small value of $(\partial d/\partial P)_T$ means that the distance between Zn-porphyrin in ZnCyt*c* and heme in Cytb_5 results in the order of 0.1 Å reduction at 200 MPa, to the extent of which the ZnCyt*c*/Cytb_5 complex structure would be little perturbed by pressurization. If the shift of the binding site was induced by pressure, the distance change estimated by the ET rate constants might be more significant. It can be well considered that the binding geometry remains unchanged in the pressure range (0.1−200 MPa), on the basis of which we will discuss the interaction between ZnCyt*c* and Cytb_5 in the next section.

DISCUSSION

Pressure dependence of the ET kinetics in the ZnCyt*c*/ferric Cytb_5 complex resulted in a volume change, ΔV_d^{Zn}, of −8.5 cm^3 mol^{-1} upon its dissociation, which is considerably smaller compared to the previous data on the ferric pair of the Cyt*c* and Cytb_5 proteins, −122 cm^3 mol^{-1} (ΔV_d^{Fe}) (*16*), despite the same solution condition, 2 mM Tris-HCl, pH 7.4, and the same protein species, horse heart Cyt*c* and rat hepatic Cytb_5. The method to monitor the dissociation of the Cyt*c*/Cytb_5 complex is one of the different points between the present and the previous studies (*16*); the previous ΔV_d^{Fe} was monitored by the perturbation of the Cytb_5 absorption spectrum upon its complexation with Cyt*c*. In the case of the Cyt*c*/Cytb_5 complex, these two methods, i.e., the ET kinetics and the absorption spectrum, are suggested to be comparable for the evaluation of its dissociation constant (*40*), and therefore a much smaller ΔV_d^{Zn} than ΔV_d^{Fe} is not due to the different techniques to monitor the protein−protein interactions.

As mentioned in Introduction, dissociation of protein−protein complexes usually accompanies the volume change, and its degree is characteristic of the type of the interactions in its complexes (*13*, *14*). Accordingly, the simplest explanation for the smaller value of ΔV_d^{Zn} than the previously reported ΔV_d^{Fe} is that ZnCyt*c* does not interact with ferric Cytb_5 in the same manner as ferric Cyt*c* does.

Electrostatic Interactions: Salt Bridge Formations. In the complex between ferric Cyt*c* and ferric Cytb_5, ΔV_d^{Fe} of −122 cm^3 mol^{-1} has been well interpreted as the rupture of four salt bridge interactions on the basis of the −10 to −30 cm^3 mol^{-1} contribution from one salt bridge dissociation. If ΔV_d^{Zn} results from the salt bridge interaction alone, at most one salt bridge would be formed on their complexation. Because salt bridge interaction depends on the electrostatic properties on protein surface (*41*−*45*), Zn substitution could lead to perturbation on the electrostatic potential of the Cyt*c* protein surface and result in the different interaction with Cytb_5 between ferric Cyt*c* and ZnCyt*c*. Affinity between the electrostatically stabilized protein pairs is influenced especially by the net charge and dipole moment of protein molecules (*41*, *42*). The zinc substitution for ferric iron in Cyt*c* decreases its net charge from +8.1 to +7.1 and the magnitude of the dipole moment of the overall protein from 225 to 195 D[3]. In ZnCyt*c*, reduction of the positive characters in the net charge and dipole moment could weaken the electrostatic interactions with negatively charged Cytb_5.

It is well known (*41*−*45*) that ionic strength of solution can reduce electrostatic interactions for the salt bridge formation. As reported by Mauk et al. (*46*), the dissociation constant of the ferric complex between Cyt*c* and Cytb_5 amounts to 0.25 μM in solution of 1 mM ionic strength and is increased to as much as 13 μM at 10 mM ionic strength (*46*), which is consistent with the presence of the salt bridge interactions between ferric Cyt*c* and ferric Cytb_5. In the present ZnCyt*c*/Cytb_5 complex, K_d^{Zn} at 2 mM Tris-HCl buffer concentration was 1.5 μM (Figure 3A). Compared to the ferric Cyt*c*/Cytb_5 complex (K_d of 0.25 μM), a reduced affinity between ZnCyt*c* and Cytb_5 might be due to the decline in the positive characters of the surface on Cyt*c* by the Zn-substitution. Nonetheless, increasing the buffer concentration to 10 mM led to the 10-fold increase in K_d^{Zn}, 12 μM. Although it remains unclear whether the specific salt bridges proposed in the ferric pair exist in the ZnCyt*c*/Cytb_5 complex, the significant dependence of K_d^{Zn} on ionic strength indicates the importance of the electrostatic interactions in formation of the ZnCyt*c*/Cytb_5 complex. On the basis of the ionic strength dependence of K_d^{Zn}, ΔV_d^{Zn} is expected to be comparable to ΔV_d^{Fe}, −122 cm^3 mol^{-1}, but the observed ΔV_d^{Zn} was much smaller (−8.5 cm^3 mol^{-1}). Therefore, in addition to salt bridge interactions, the ZnCyt*c*/Cytb_5 complex is supposed to have some other interactions with the positive volume change upon its disruption, and such interactions are not available in the ferric Cyt*c*/ferric Cytb_5 complex.

Hydrogen-Bonding Interactions. Other than salt bridge interaction, it has been recognized that hydrogen bonding and hydrophobic interactions also stabilize protein−protein complexes. The volume change, ΔV_d^{H-bond}, caused by disruption of hydrogen bonding interaction appears to be positive (*13*, *14*). Czeslik and Jonas (*47*) have estimated ΔV_d^{H-bond} of about +1.75 cm^3 mol^{-1} per one hydrogen bonding interaction by examining the pressure dependence of the hydroxyl proton chemical shift of methanol in the monomer−tetramer equilibrium using high-pressure ^{1}H NMR. Compared to the large decrease in volume, −10 to −30 cm^3 mol^{-1}, of one salt bridge dissociation, the small positive value of ΔV_d^{H-bond}, +1.75 cm^3 mol^{-1}, is considered

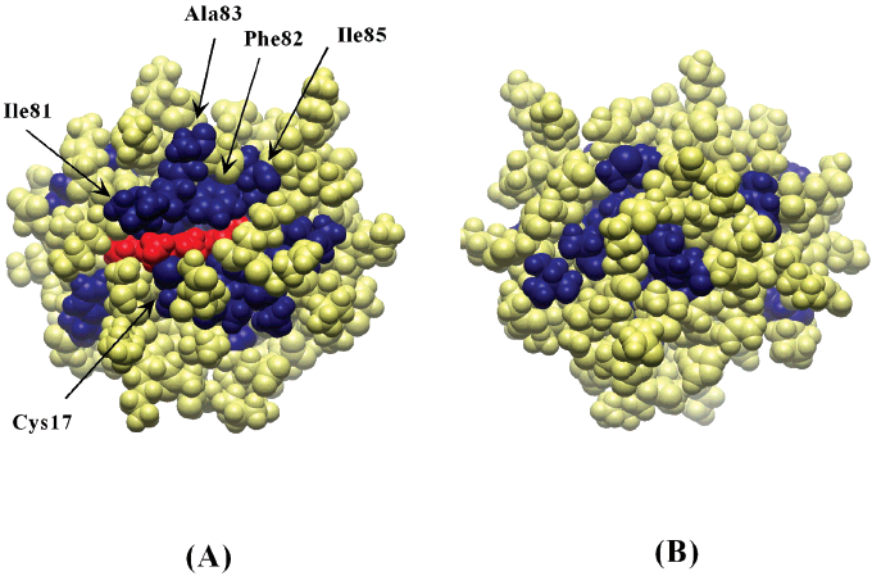

FIGURE 6: Distribution of the hydrophobic residues on the surface of ferrous Cyt*c* represented by CPK model. Hydrophobic residues and heme are colored by blue and red, respectively. A is from the side near heme, while the figure from the opposite side are shown in B. The coordination of the structure was taken from the protein data bank; 1GIW of ferrous Cyt*c*.

to have a little contribution to the observed ΔV_d^{Zn} of -8.5 cm^3 mol^{-1}, and approximately 10 hydrogen bonds might be necessary to compensate the negative contribution from only one salt bridge interaction. It seems to be too many hydrogen bonds for the interaction between proteins (*48*), and the observed ΔV_d^{Zn} cannot be fully explained by taking the salt bridge and the hydrogen bonding interactions into consideration.

Hydrophobic Interactions. Another stabilizing factor, hydrophobic interaction, is also considered to exhibit the positive volume change upon its dissociation, $\Delta V_d^{hydrophobic}$, which has been often examined by the transfer of a nonpolar molecule from a nonpolar environment into aqueous solution. Prehoda and Markley (*49*) estimated that the volume change due to interaction of the hydrocarbon molecules with water is about $+0.16$ cm^3 mol^{-1} per 1 Å^2 of the nonpolar surface area. Also in protein−protein interactions, a significant positive volume change, $+50$ cm^3 mol^{-1}, has been observed (*50*) upon dissociation of the complex between digoxigenin and antidigoxin MAb 26−10, where all of the contacts are hydrophobic (*51*). On the basis of about 300 Å^2 buried area in this digoxigenin/MAb 26−10 complex, $+0.17$ cm^3 mol^{-1}Å^{-2} was evaluated for the value of $\Delta V_d^{hydrophobic}$ per 1 Å^2. Therefore, one possibility to account for much smaller value of ΔV_d^{Zn} is that hydrophobic interactions can partially cancel out the negative characters of the volume changes arising from the salt bridge interactions.

The hydrophobic interactions play an important role in the association of Cyt*c* with the other redox proteins such as Cyt*c* oxidase (*52*) and plastocyanin (*53*). As shown in Figure 6A,B, Cyt*c* has a unique hydrophobic cluster including Cys17, Ile81, Phe82, Ala83, and Ile85 (colored blue) on its surface around heme, which are further surrounded by several Lys residues to bear the positive electrostatic potential. The hydrophobic vinyl and methyl groups of heme (colored red) are also included in this hydrophobic cluster, the surface of which amounts to more than 100 Å^2 (rectangular surrounded by Cys17, Ile81, Ala83, and Ile85). In the Cyt*c*/Cyt*c* oxidase complexation process (*52*), for example,

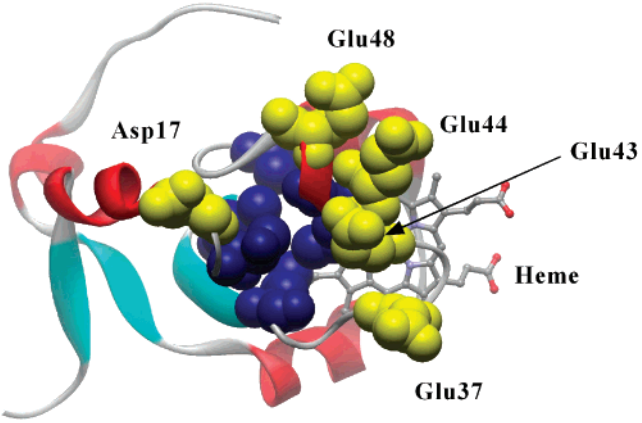

FIGURE 7: Cleft site proposed by Storch et al. (*58*) on rat hepatic Cytb_5. The hydrophobic residues which would be exposed to solvent by the cleft formation are colored blue, and the acidic residues, Asp and Glu, at the rim of the cleft are shown in yellow.

this hydrophobic cluster of Cyt*c* (Figure 6A) is in contact with the corresponding hydrophobic region of Cyt*c* oxidase with help of three or four salt bridge interactions between the positive residues (Lys) on Cyt*c* and the negative ones (Asp and Glu) on Cyt*c* oxidase. Upon dissociation of the Cyt*c*/Cyt*c* oxidase complex, approximately -100 cm^3 mol^{-1} of ΔV_d can be estimated solely on the basis of the salt bridge interactions. In contrast, positive value of ΔV_d, $+6.3$ cm^3 mol^{-1}, has been observed (*54*, *55*). Thus, the hydrophobic region on the surface of Cyt*c* is available for the binding with its redox partners, which would make the observed ΔV_d more positive than expected based upon the salt bridge interactions.

While there seems to be no hydrophobic regions on the surface of Cytb_5 to interact with the hydrophobic cluster on Cyt*c*, the recent molecular dynamics simulation on the structural fluctuation of Cytb_5 (*56*) has proposed the formation of a large cleft that exposes the hydrophobic interior and the heme group (Figure 7) to solvents. Though opening and closing of the cleft occurred in nanosecond time scale, Hom et al. (*7*) have suggested in their two-dimensional NMR

spectroscopic experiments that the hydrophobic cleft of Cytb_5 can interact with the hydrophobic cluster of the Cyt*c* surface to form the complex. As calculated by Storch et al. (*56*), the maximum dimensions of this cleft were 15.2 Å × 10.5 Å × 11.5 Å (length by width by depth). Taking 0.17 cm^3 mol^{-1}Å^{-2} of $\Delta V_d^{\text{hydrophobic}}$ into account, larger than 100 Å^2 of the hydrophobic interaction area would result in the positive contribution of $>+20$ cm^3 mol^{-1} to the volume change. In this binding geometry, there are also at least two intermolecular salt bridge interactions: Glu10(Cytb_5)−Lys27(Cyt*c*) and Glu43(Cytb_5)−Lys72(Cyt*c*). Besides approximately +20 cm^3 mol^{-1} of $\Delta V_d^{\text{hydrophobic}}$, these two salt bridges would further negatively contribute to the volume change of −20 to −60 cm^3 mol^{-1} upon the complex dissociation, resulting in the small ΔV_d^{Zn}, −8.5 cm^3 mol^{-1}. While further studies are necessary to prove whether the cleft model is indeed realized in the present ZnCyt*c*/Cytb_5 complex, the cleft binding model with the considerable hydrophobic interactions would be reasonable to account for the observed ΔV_d^{Zn}.

As reported in the two-dimensional NMR study (*27*), ZnCyt*c* has been assumed to be the structural model of ferrous Cyt*c* probably including its dynamical features. Moreover, ferric and ferrous Cyt*c* have virtually the same backbone conformations, and ferric Cyt*c* displays larger-amplitude motions than the ferrous form (*19*, *57*). Although the structural features of ZnCyt*c* including its dynamics should be clarified especially in relation to those of ferric Cyt*c* by future studies in more detail, ferric Cyt*c* might show a larger dynamical behavior compared to ZnCyt*c*. Difference in the amplitudes of structural dynamics in protein imply the temporal difference of the atomic coordinates of amino acid residues, which could further influence on the geometries of protein complexes. Indeed, when one of the four salt bridge interactions (heme propionate in Cytb_5 and Lys79 on Cyt*c*, Figure 1) is disrupted by esterification of the heme propionate in Cytb_5, electrostatic calculations combined with equilibrium binding measurements have suggested (*26*) that Cyt*c* forms a complex with esterified-Cytb_5 at the different site from that of native Cytb_5. In addition, one of the salt-bridging residues in Salemme model, Lys13, on Cyt*c* has been proposed to be related to the oxidation-state-dependent affinities between Cyt*c* and Cyt*c* oxidase (*58*). Depending on the Cyt*c* oxidation states, the perturbation of only one salt bridge appears to be enough for the alteration of the docking geometries between cytochromes *c* and b_5, hydrophobic ZnCyt*c*/Cytb_5 and electrostatic ferric Cyt*c*/Cytb_5 interactions. While the hydrophobic interaction in the ZnCyt*c*/Cytb_5 complex is needed to be directly detected in the future studies, oxidation-state-dependent change in the Cyt*c*/Cytb_5 binding geometry could be induced by perturbation on only one salt bridge in response to the changes in the structural dynamics of Cyt*c*.

ACKNOWLEDGMENT

We are grateful to Professor Stephen G. Sligar (University of Illinois) for a gift of the expression vector of the rat hepatic cytochrome b_5 gene and to Professor Saburo Aimoto (Osaka University) for the preparation of ZnCyt*c*. We are also obliged to Dr. Satoshi Takahashi (Kyoto University) for the fruitful discussion and to Mr. Eric Kawamoto (Northwestern University) for the proofreading of our manuscript.

SUPPORTING INFORMATION AVAILABLE

A figure of the plots of the rate constant, k_S, against the Cytb_5 concentration under 2 and 10 mM Tris-HCl, pH 7.4. This material is available free of charge via the Internet at http://pubs.acs.org.

REFERENCES

1. Marcus, R. A., and Sutin, N. (1985) *Biochim. Biophys. Acta 811*, 265−322.
2. McLendon, G., and Hake, R. (1992) *Chem. Rev. 92*, 481−490.
3. Mauk, A. G., Mauk, M. R., Moore, G. R., and Northrup, S. H. (1995) *J. Bioenerg. Biomembr. 27*, 311−330.
4. Durham, B., Fairris, J. L., McLean, M., Millet, F., Scott, J. R., Sligar, S. G., and Willie, A. (1995) *J. Bioenerg. Biomembr. 27*, 331−340.
5. Wendoloski, J. J., Matthew, J. B., Weber, P. C., and Salemme, F. R. (1987) *Science 238*, 794−797.
6. Guillemette, J. G., Barker, P. D., Eltis, L. D., Lo, T. P., Smith, M., Brayer, G. D., and Mauk, A. G. (1994) *Biochimie 76*, 592−604.
7. Hom, K., Ma, Q. F., Wolfe, G., Zhang, H., Storch, E. M., Daggett, V., Basus, V. J., and Waskell, L. (2000) *Biochemistry 39*, 14025−14039.
8. Ng, S., Smith, M. B., Smith, H. T., and Millett, F. (1977) *Biochemistry 16*, 4975−4978.
9. Burch, A. M., Rigby, S. E., Funk, W. D., MacGillivray, R. T., Mauk, M. R., Mauk, A. G., and Moore, G. R. (1990) *Science 247*, 831−3.
10. Northrup, S. H., Thomasson, K. A., Miller, C. M., Barker, P. D., Eltis, L. D., Guillemette, J. G., Inglis, S. C., and Mauk, A. G. (1993) *Biochemistry 32*, 6613−6623.
11. Willie, A., McLean, M., Liu, R. Q., Hilgen-Willis, S., Saunders, A. J., Pielak, G. J., Sligar, S. G., Durham, B., and Millett, F. (1993) *Biochemistry 32*, 7519−7525.
12. Sun, Y., Wang, Y., Yan, M., Sun, B., Xie, Y., Huang, Z., Jiang, S., and Wu, H. (1999) *J. Mol. Biol. 285*, 347−359.
13. Drljaca, A., Hubbard, C. D., van Eldik, R., Asano, T., Basilevsky, M. V., and le Noble, W. J. (1998) *Chem. Rev. 98*, 2167−2289.
14. Mozhaev, V. V., Heremans, K., Frank, J., Masson, P., and Balny, C. (1996) *Proteins: Struc., Funct., Genet. 24*, 81−91.
15. Rodgers, K. K., Pochapsky, T. C., and Sligar, S. G. (1988) *Science 240*, 1657−1659.
16. Rodgers, K. K., and Sligar, S. G. (1991) *J. Mol. Biol. 221*, 1453−1460.
17. Salemme, F. R. (1976) *J. Mol. Biol. 102*, 563−568.
18. Qi, P. X., Beckman, R. A., and Wand, A. J. (1996) *Biochemistry 35*, 12275−12286.
19. Banci, L., Bertini, I., Huber, J. G., Spyroulias, G. A., and Turano, P. (1999) *J. Biol. Inorg. Chem. 4*, 21−31.
20. Berghuis, A. M., and Brayer, G. D. (1992) *J. Mol. Biol. 223*, 959−976.
21. Trewhella, J., Carlson, V. A., Curtis, E. H., and Heidorn, D. B. (1988) *Biochemistry 27*, 1121−1125.
22. Calvert, J. F., Hill, J. L., and Dong, A. (1997) *Arch. Biochem. Biophys. 346*, 287−293.
23. Frolov, E. N., Gvosdev, R., Goldanskii, V. I., and Parak, F. G. (1997) *J. Biol. Inorg. Chem. 2*, 710−713.
24. Kornblatt, J. A., and Luu, H. A. (1986) *Eur. J. Biochem. 159*, 407−413.
25. Hake, R., McLendon, G., Corin, A., and Holzschu, D. (1992) *J. Am. Chem. Soc. 114*, 5442−5443.
26. Mauk, M. R., Mauk, A. G., Weber, P. C., and Matthew, J. B. (1986) *Biochemistry 25*, 7085−7091.
27. Anni, H., Vanderkooi, J. M., and Mayne, L. (1995) *Biochemistry 34*, 5744−5753.
28. Qin, L., and Kostic, N. M. (1994) *Biochemistry 33*, 12592−12599.
29. von Bodman, S. B., Schuler, M. A., Jollie, D. R., and Sligar, S. G. (1986) *Proc. Natl. Acad. Sci. U.S.A. 83*, 9443−9447.
30. Vanderkooi, J. M., Adar, F., and Erecinska, M. (1976) *Eur. J. Biochem. 64*, 381−387.
31. Newmann, R. C., Jr., Kauzmann, W., and Zipp, A. (1973) *J. Phys. Chem. 77*, 2687−2691.
32. McLendon, G., and Miller, J. R. (1985) *J. Am. Chem. Soc. 107*, 7811−7816.

33. McLendon, G. L., Winkler, J. R., Nocera, D. G., Mauk, M. R., Mauk, A. G., and Gray, H. B. (1985) *J. Am. Chem. Soc. 107*, 739−740.
34. Furukawa, Y., Ishimori, K., and Morishima, I. (2000) *J. Phys. Chem. B 104*, 1817−1825.
35. Miyashita, O., and Go, N. (1999) *J. Phys. Chem. B 103*, 562−571.
36. Sun, J., Wishart, J. F., van Eldik, R., Shalders, R. D., and Swaddle, T. W. (1995) *J. Am. Chem. Soc. 117*, 2600−2605.
37. Scott, J. R., Fairris, J. L., McLean, M., Wang, K., Sligar, S. G., Durham, B., and Millett, F. (1996) *Inorg. Chim. Acta 243*, 193−200.
38. Feitelson, J., and Mauzerall, D. (1996) *J. Phys. Chem. 100*, 7698−7703.
39. Winkler, J. R., and Gray, H. B. (1992) *Chem. Rev. 92*, 369−379.
40. Willie, A., Stayton, P. S., Sligar, S. G., Durham, B., and Millett, F. (1992) *Biochemistry 31*, 7237−7242.
41. van Leeuwen, J. W. (1983) *Biochim. Biophys. Acta 743*, 408−421.
42. Watkins, J. A., Cusanovich, M. A., Meyer, T. E., and Tollin, G. (1994) *Protein Sci. 3*, 2104−2114.
43. Meyer, T. E., Rivera, M., Walker, F. A., Mauk, M. R., Mauk, A. G., Cusanovich, M. A., and Tollin, G. (1993) *Biochemistry 32*, 622−627.
44. Meyer, T. E., Watkins, J. A., Przysiecki, C. T., Tollin, G., and Cusanovich, M. A. (1984) *Biochemistry 23*, 4761−4767.
45. Cheddar, G., Meyer, T. E., Cusanovich, M. A., Stout, C. D., and Tollin, G. (1989) *Biochemistry 28*, 6318−6322.
46. Mauk, M. R., Reid, L. S., and Mauk, A. G. (1982) *Biochemistry 21*, 1843−1846.
47. Czeslik, C., and Jonas, J. (1999) *Chem. Phys. Lett. 302*, 633−638.
48. Stites, W. E. (1997) *Chem. Rev. 97*, 1233−1250.
49. Prehoda, K. E., and Markley, J. L. (1996) in *High-Pressure Effects in Molecular Biophysics and Enzymology* (Markley, J. L., Northrop, D. B., and Royer, C. A., Eds.) pp 33−43, Oxford University Press, New York.
50. Roy, P., Roth, C. M., Margolies, M. N., and Yarmush, M. L. (1999) *Mol. Immun. 36*, 1149−1158.
51. Jeffrey, P. D., Strong, R. K., Sieker, L. C., Chang, C. Y. Y., Campbell, R. L., Petsko, G. A., Haber, E., Margolies, M. N., and Sheriff, S. (1993) *Proc. Natl. Acad. Sci. U.S.A. 90*, 10310−10314.
52. Roberts, V. A., and Pique, M. E. (1999) *J. Biol. Chem. 274*, 38051−38060.
53. Qin, L., and Kostić, N. M. (1996) *Biochemistry 35*, 3379−3386.
54. Kornblatt, J. A., Hui Bon Hoa, G., and English, A. M. (1984) *Biochemistry 23*, 5906−5911.
55. Kornblatt, J. A., Theodorakis, J., Hui Bon Hoa, G., and Margoliash, E. (1992) *Biochem. Cell Biol. 70*, 539−547.
56. Storch, E. M., and Daggett, V. (1995) *Biochemistry 34*, 9682−9693.
57. Banci, L., Bertini, I., Gray, H. B., Luchinat, C., Reddig, T., Rosato, A., and Turano, P. (1997) *Biochemistry 36*, 9867−9877.
58. Falk, K. E., and Ångstrom, J. (1983) *Biochim. Biophys. Acta 722*, 291−296.

BI0257890